Room-temperature lasing of electrically pumped red-emitting InP / (Al 0.20 Ga 0.80) 0.51 In 0.49 P quantum dots embedded in a vertical microcavity

Marcus Eichfelder, Wolfgang-Michael Schulz, Matthias Reischle, Michael Wiesner, Robert Roßbach, Michael Jetter, and Peter Michler

Citation: Applied Physics Letters **95**, 131107 (2009); doi: 10.1063/1.3236752
View online: http://dx.doi.org/10.1063/1.3236752
View Table of Contents: http://scitation.aip.org/content/aip/journal/apl/95/13?ver=pdfcov
Published by the AIP Publishing

Room-temperature lasing of electrically pumped red-emitting InP/$(Al_{0.20}Ga_{0.80})_{0.51}In_{0.49}P$ quantum dots embedded in a vertical microcavity

Marcus Eichfelder,[a] Wolfgang-Michael Schulz, Matthias Reischle, Michael Wiesner, Robert Roßbach, Michael Jetter, and Peter Michler
Institut für Halbleiteroptik und Funktionelle Grenzflächen, Universität Stuttgart, Allmandring 3, 70569 Stuttgart, Germany

(Received 5 March 2009; accepted 11 August 2009; published online 29 September 2009)

We demonstrate electrically pumped laser light emission in the visible (red) spectral range using self-assembled InP quantum dots embedded in a microcavity mesa realized by monolithically grown high-reflectivity AlGaAs distributed Bragg reflectors. We used common semiconductor laser processing steps to fabricate stand-alone index-guided vertical-cavity surface-emitting lasers with oxide apertures for optical wave-guiding and electrical current constriction. Ultra-low threshold of around 10 A/cm^2 and room temperature lasing were demonstrated. Additionally, the temperature independence of the threshold current, which was predicted in theory for quantum dot lasers, is displayed. © *2009 American Institute of Physics*. [doi:10.1063/1.3236752]

High-quality solid-state emitters have proven to be very attractive light sources. Beyond Fabry–Pérot semiconductor resonators, microdisk structures[1] and photonic-crystal microcavities, vertical-cavity surface-emitting lasers (VCSELs) (Ref. 2) provide ultra-low threshold operation even in the submilliampere regime[3] and high-speed modulation capability. Additionally, the easy coupling to optical fibers and on-wafer processing are attractive features. For a laser device with low threshold current, it is essential to decrease the pumped mode volume by using an oxide aperture above the cavity[4] and thereby decreasing the active volume for lowest power consumption. By using zero-dimensional quantum dots (QDs) as the active medium of semiconductor lasers, theory has predicted splendid properties compared to higher dimensional media,[5,6] such as low thresholds and broader gain spectra. In the In(Ga)As/GaAs material system, laser physics and development have reached a high level and are best understood.[7] In Ref. 3, the authors showed low threshold current densities J_{th} of around 113 A/cm^2 for micropillar lasers in the InGaAs/GaAs material system with a QD density of 5×10^9 cm^{-2}. World record transparency current density value of 6 A/cm^2 for one QD layer with a QD density of 1×10^{11} cm^{-2} in the InGaAs/GaAs material system was reached by the authors in Ref. 8. It is also preferable to fabricate QDs at shorter wavelengths as active emitters for on-board optical interconnects and polymer optical fiber (POF) applications as common avalanche photodiodes have their highest photon detection efficiency in the red spectral range. However, for any kind of data communication via POF, transmission in the spectral window around 650 nm is desirable.[9] For adequate usage of the laser, operation at room temperature and above is required. Quantum well VCSELs in the same spectral region and GaInP/AlGaInP material system exhibit low J_{th} values in the range of around 2 kA/cm^2 at 293 K.[10] For InP/GaInP QDs as active layer for edge-emitting lasers, J_{th} values of around 288 A/cm^2 at 90 K were reached.[11]

In this letter, we report on electrically pumped InP QDs embedded in a microcavity *p-i-n* diode structure showing laser action at 290 K. The effect of oxide-aperture diameter on the appearance of optical transverse modes is also investigated. Furthermore, we show the temperature dependent J_{th} being nearly constant as predicted from theory.[6]

The sample structure was fabricated by metal-organic vapor-phase epitaxy (MOVPE) with standard sources at low pressure (100 mbar) on (100) GaAs substrates oriented 6° toward the [111]*A* direction. The *n*-type distributed Bragg reflector (DBR) consists of 45 $\lambda/4$ pairs of $Al_{0.50}GaAs:Si/AlAs:Si$ grown at 750 °C. The single layer of self-assembled InP QDs was grown using the Stranski–Krastanow growth mode[12] by depositing 2.1 ML of InP at 650 °C and a growth rate of 1.05 ML/s. The QDs were fabricated on $(Al_{0.20}Ga_{0.80})_{0.51}In_{0.49}P$ as barrier material in the center of a one-wavelength-thick $(Al_{0.55}Ga_{0.45})_{0.51}In_{0.49}P$ cavity spacer which is lattice matched to GaAs.[13] The growth was interrupted for 20 s directly after the deposition of the QDs in order to ripen the QDs. Atomic force microscope measurements were used to determine the surface density of the QDs (5.5×10^{10} cm^{-2}). To form a current aperture for electrical pumping, an $Al_{0.98}GaAs$ oxidation layer was inserted above the cavity. The oxide aperture leads to a number of QDs from 5×10^3 to 1×10^5 lying spatially under the respective aperture opening while the pumped volume is expected to be larger due to current spreading between the active region and the current constriction layer. Later on, the three investigated VCSELs are labeled according to their size of oxide aperture diameter as follows: VCSEL 1 (15.7 μm), VCSEL 2 (9 μm), and VCSEL 3 (2×5.7 μm, minor and major axis of the elliptical aperture). The unintentional elliptical shape of the oxide aperture of VCSEL 3 is a result of small imperfections of the processing technology. For VCSELs, the gain region is very short requiring high reflective mirrors to reach threshold. With these DBRs, high quality factors and thus long photon lifetimes within the cavity are

[a]Electronic mail: m.eichfelder@ihfg.uni-stuttgart.de. URL: http://www.ihfg.uni-stuttgart.de.

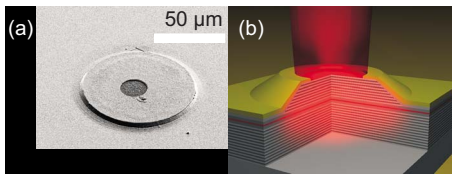

FIG. 1. (Color online) (a) SEM image and (b) scheme of a cross section of the structured microcavity with the embedded InP-QD layer as active region colored in red.

achieved. A strong carrier confinement due to an increased barrier height helps to confine carriers in the dots and minimize possible leakage current which would cause an additional internal temperature rise. A *p*-type top DBR consisting of 36 $\lambda/4$ pairs of $Al_{0.50}GaAs:C/Al_{0.95}GaAs:C$ with linearly graded interfaces grown at 750 °C finalized the microcavity.[14] The temperature change during the QD growth does not affect the growth of the top DBR.[15] The cavity was designed to have a normal-incidence cavity resonance at around 1.9 eV at 290 K. The complete growth was *in situ* monitored by LayTec's EpiR-M *in situ* reflection measurement setup.[16] The mesa microcavity was also investigated using a scanning electron microscope (SEM), as shown in Fig. 1(a). A scheme of our device layout is shown in Fig. 1(b). Postgrowth standard lithography, wet oxidation, and evaporation of ohmic contacts were used to fabricate single devices. A ring contact with 20 μm opening window was used for current injection through the upper DBR.

Temperature-dependent electroluminescence (EL) experiments were performed using a related setup as described in Ref. 15. A direct current (dc) power source was used as the electric pump source.

An overview spectrum in Fig. 2(a) shows the laser emission line at 290 K due to the cavity resonance positioned at 1.9 eV for VCSEL 1 which is blue detuned with respect to the QD ensemble. A high spectral resolution EL measurement of the above mentioned sharp laser line reveals a large number of higher transverse modes on the high energy side of the fundamental mode as shown in Fig. 2(b). As the aperture diameter is reduced to 9 μm, as shown in Fig. 2(c), the high resolution measurement reveals a smaller number of

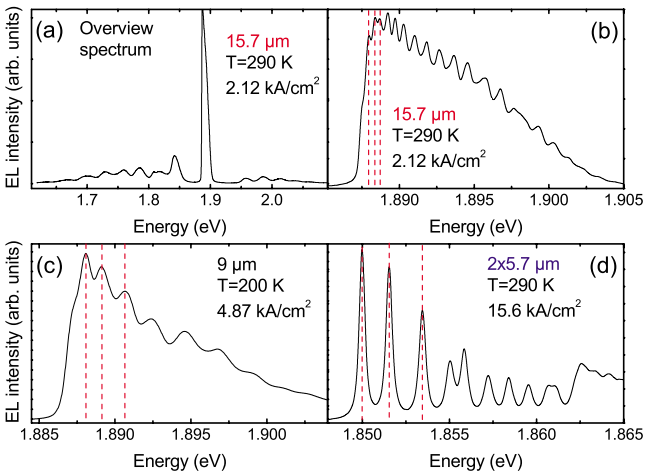

FIG. 2. (Color online) (a) Overview spectrum of VCSEL 1 showing lasing action at a drive current of 2.12 kA/cm^2 at 290 K. [(b)–(d)] High spectral resolution EL measurements of VCSEL 1, 2 and 3. The different peak position in energy for each laser is mainly due to different positions on the wafer. The dashed vertical lines are guide to the eye and marking the position of the fundamental mode and two transverse modes.

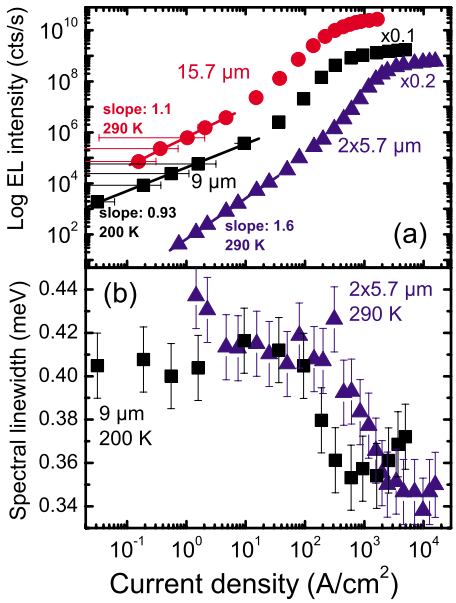

FIG. 3. (Color online) (a) Integrated intensities over all modes for VCSEL 1, 2 and 3 under dc electrical excitation at 290 K. The superlinear regime around J_{th} of 10 A/cm^2 is a strong hint on lasing. Additionally, we want to point out the extremely high count rates easily exceeding 5×10^{10} counts/s for VCSEL 1. The data for the VCSEL 2 and 3 are both offset by a factor.(b) The linewidth of the fundamental mode with increasing current density is shown here for two devices.

higher transverse modes. In addition, the splitting between the modes is increased in comparison to the 15.7 μm aperture. The quality factor Q of the cavity can be determined from the linewidth of the fundamental mode at transparency yielding a value of 4500. A further reduction of the aperture diameter to an elliptically shaped 2×5.7 μm^2 aperture displays the general indication that the number of transverse modes are further decreased. A trend is observed with reduced aperture diameter. The number of transverse modes is decreased and the mode splitting between the fundamental mode and higher order modes is enhanced. In fact, these two effects are known from micropillar lasers for different pillar diameters as it was shown in Refs. 17 and 18. We did not observe an obvious mode splitting from the laser with the elliptically shaped aperture as one would expect,[19] which might be due to increased scattering losses[20] affecting the mode component associated with the minor axis of the elliptically shaped oxide aperture. On the other hand, the absence of mode splitting could also be attributed to an asymmetric current flow due to the misoriented substrate.[21] Therefore, we expect the mode spacing to be dominated by the large axis of the oxide aperture of VCSEL 3. In comparison, another device with a circular shaped 2.4 μm aperture showed a distinct enlarged mode spacing compared to VCSEL 3 (data not shown here).

The input-output characteristics of the three devices are given in Fig. 3(a). While lasing action was observed for VCSEL 1 and 3 at room temperature, VCSEL 2 showed lasing up to 200 K, which might be due to imperfections in the laser fabrication process. As the current density is continuously increased from 1×10^{-4} to around 10 A/cm^2 in Fig. 3(a), the integrated intensity over all modes increases linearly. The further increase in current density results in a superlinear increase in integrated intensity whose position we identify as J_{th} of our laser. Finally, even higher current densities result in saturation of output power. The error bars for the integrated

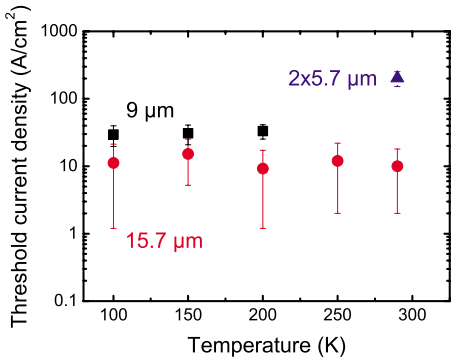

FIG. 4. (Color online) J_{th} of VCSEL 1, 2 and 3 as a function of temperature. The measurement of our three devices shows that J_{th} is nearly constant over the investigated temperature range.

intensity do not appear in the diagram as they are in the range of ±5%. While the aperture diameter is reduced to 9 μm, J_{th} is increased to around 32 A/cm^2 and the maximum output power decreases. This can be explained due to the fact that the number of QDs, which match optically and spatially to the mode is reduced and underlies the probability to be under the electrically pumped area. For VCSEL 3, J_{th} further increases to around 200 A/cm^2 and the obtained optical output power is obviously much smaller. This is due to the smaller active volume. At the current stage of development, we estimate the overall efficiency of VCSEL 1 to be below 1%.

Another strong indication of lasing is the linewidth sharpening by increasing current injection.[22] For this purpose we investigated the linewidth of VCSEL 2 at 200 K and VCSEL 3 at room temperature as shown in Fig. 3(b). As the mode spacing is very small for VCSEL 1, we could not extract the linewidth behavior as a function of current density in this case. By increasing current density to 200 A/cm^2, the linewidth stays nearly constant within the error bars for the smallest aperture. A further increase in pump power results in a linear decrease of the spectral linewidth. This linewidth narrowing agrees well with the nonlinear intensity increase of VCSEL 2 and 3 given in Fig. 3(a). The further spectral linewidth narrowing can be understood as a consequence of a rising coherence inside the laser cavity.[23] An increase of the current density above 310 A/cm^2 results in spectral linewidth narrowing down to 0.34 meV. If the injection current is further increased, the linewidth starts to broaden again due to current induced thermal effects. VCSEL 2 shows a similar spectral linewidth behavior being investigated at 200 K.

Finally, J_{th} was evaluated out of Fig. 3(a) for temperatures in a range from 100 to 290 K. The results are shown in Fig. 4. It appears that the J_{th} is nearly temperature independent which might originate from a broad gain contribution of the QD ensemble in general and besides from three-dimensional carrier confinement as predicted.[6] Also, lowest J_{th} values of around 10–30 A/cm^2 were observed. The increase in J_{th} for reduced aperture diameters might be correlated with nonradiative losses and scattering losses.[20]

In the end, we want to discuss the investigations we made concerning the number of QDs contributing to emission of coherent light. 5×10^3 to 1×10^5 QDs are lying spatially under the aperture opening while the number of QDs that match spectrally to the cavity resonance is between around 7 and 160. This is due to the large QD ensemble with its broad emission spectra of around 170 meV and cavity detuning being in a range of around 114 meV at 300 K. The surprising effect that such a small number of QDs can exhibit enough gain to lasing might be explained by nonresonant dot-cavity coupling mechanisms.[24,25] In Ref. 25, the authors showed in detail that two to four QDs in a photonic crystal cavity being optically pumped provide sufficient gain for lasing and they reason that with cooperation from the surrounding nonresonant QDs emission into the lasing mode becomes feasible. In this case, a perfect spectral dot-cavity alignment is not essentially needed but a reduced detuning might help to improve the performance of future devices.

In this letter, we demonstrated lasing of red InP/$(Al_{0.20}Ga_{0.80})_{0.51}In_{0.49}P$ QD VCSEL which have been electrically pumped. Mode behavior, input/output characteristics and spectral linewidth formation above threshold have been investigated. Finally, the temperature dependence of the J_{th} was investigated. Hardly any comparable values like the threshold current density of 10 A/cm^2 can be found in literature in this material system.

[1] P. Michler, A. Kiraz, L. Zhang, C. Becher, E. Hu, and A. Imamoglu, Appl. Phys. Lett. **77**, 184 (2000).
[2] K. Iga, IEEE J. Sel. Top. Quantum Electron. **6**, 1201 (2000).
[3] S. Reitzenstein, T. Heindel, C. Kistner, A. Rahimi-Iman, C. Schneider, S. Höfling, and A. Forchel, Appl. Phys. Lett. **93**, 061104 (2008).
[4] K. Iga, Jpn. J. Appl. Phys. **47**, 1 (2008).
[5] M. Asada, Y. Miyamoto, and Y. Suematsu, IEEE J. Quantum Electron. **22**, 1915 (1986).
[6] Y. Arakawa and H. Sakaki, Appl. Phys. Lett. **40**, 939 (1982).
[7] D. Bimberg, J. Phys. D: Appl. Phys. **38**, 2055 (2005).
[8] R. L. Sellin, Ch. Ribbat, M. Grundmann, N. N. Ledentsov, and D. Bimberg, Appl. Phys. Lett. **78**, 1207 (2001).
[9] H. P. A. van den Boom, W. Li, P. K. van Bennekom, I. T. Monroy, and G.-D. Khoe, IEEE J. Sel. Top. Quantum Electron. **7**, 461 (2001).
[10] T. Calvert, B. Corbett, and J. D. Lambkin, Electron. Lett. **38**, 222 (2002).
[11] J. Porsche, M. Ost, F. Scholz, A. Fantini, F. Phillipp, T. Riedl, and A. Hangleiter, IEEE J. Sel. Top. Quantum Electron. **6** No. 3, 482 (2000).
[12] I. N. Stranski and L. Krastanow, AMA Arch. Ophthalmol. **146**, 797 (1938).
[13] W.-M. Schulz, R. Roßbach, M. Reischle, G. J. Beirne, M. Bommer, M. Jetter, and P. Michler, Phys. Rev. B **79**, 035329 (2009).
[14] R. P. Schneider, J. A. Lott, K. L. Lear, K. D. Choquette, M. H. Crawford, S. P. Kilcoyne, and J. J. Figiel, J. Cryst. Growth **145**, 838 (1994).
[15] R. Roßbach, M. Reischle, G. J. Beirne, M. Jetter, and P. Michler, Appl. Phys. Lett. **92**, 071105 (2008).
[16] LayTec GmbH, www.laytec.de.
[17] M. Benyoucef, S. M. Ulrich, P. Michler, J. Wiersig, F. Jahnke, and A. Forchel, N. J. Phys. **6**, 91 (2004).
[18] M. Bayer, A. Forchel, Th. L. Reinecke, P. A. Knipp, and S. Rudin, Phys. Status Solidi A **191** No. 1, 3 (2002).
[19] B. Gayral, J. M. Gérard, B. Legrand, E. Costard, and V. Thierry-Mieg, Appl. Phys. Lett. **72**, 1421 (1998).
[20] E. R. Hegblom, D. I. Babic, B. J. Thibeault, and L. A. Coldren, IEEE J. Sel. Top. Quantum Electron. **3**, 379 (1997).
[21] J. E. Chung, J. Chen, P.-K. Ko, C. Hu, and M. Levi, IEEE Trans. Electron Devices **38** No. 3, 627 (1991).
[22] C. H. Henry, IEEE J. Quantum Electron. **18**, 259 (1982).
[23] S. Ates, C. Gies, S. M. Ulrich, J. Wiersig, S. Reitzenstein, A. Löffler, A. Forchel, F. Jahnke, and P. Michler, Phys. Rev. B **78**, 155319 (2008).
[24] M. Kaniber, A. Laucht, A. Neumann, J. M. Villas-Bôas, M. Bichler, M.-C. Amann, and J. J. Finley, Phys. Rev. B **77**, 161303(R) (2008).
[25] S. Strauf, K. Hennessy, M. T. Rakher, Y.-S. Choi, A. Badolato, L. C. Andreani, E. L. Hu, P. M. Petroff, and D. Bouwmeester, Phys. Rev. Lett. **96**, 127404 (2006).